Mechanics & Industry **21**, 619 (2020)

https://doi.org/10.1051/meca/2020091

Mechanics & Industry

Available online at:
www.mechanics-industry.org

Regular Article

Ball bearing turbocharger vibration management: application on high speed balancer

Kostandin Gjika[1,*], Antoine Costeux[1], Gerry LaRue[2], and John Wilson[2]

[1] Garrett-Advancing Motion, ZI Inova 3000, 2 Rue de l'Avenir, Thaon-les-Vosges, Capavenir Vosges 88155, France
[2] Garrett-Advancing Motion, 2525 W 190th St., Torrance, CA 90504, USA

Received: 18 July 2020 / Accepted: 19 November 2020

Abstract. Today's modern internal combustion engines are increasingly focused on downsizing, high fuel efficiency and low emissions, which requires appropriate design and technology of turbocharger bearing systems. Automotive turbochargers operate faster and with strong engine excitation; vibration management is becoming a challenge and manufacturers are increasingly focusing on the design of low vibration and high-performance balancing technology. This paper discusses the synchronous vibration management of the ball bearing cartridge turbocharger on high-speed balancer and it is a continuation of papers [1–3]. In a first step, the synchronous rotordynamics behavior is identified. A prediction code is developed to calculate the static and dynamic performance of "ball bearing cartridge-squeeze film damper". The dynamic behavior of balls is modeled by a spring with stiffness calculated from Tedric Harris formulas and the damping is considered null. The squeeze film damper model is derived from the Osborne Reynolds equation for incompressible and synchronous fluid loading; the stiffness and damping coefficients are calculated assuming that the bearing is infinitely short, and the oil film pressure is modeled as a cavitated π film model. The stiffness and damping coefficients are integrated on a rotordynamics code and the bearing loads are calculated by converging with the bearing eccentricity ratio. In a second step, a finite element structural dynamics model is built for the system "turbocharger housing-high speed balancer fixture" and validated by experimental frequency response functions. In the last step, the rotating dynamic bearing loads on the squeeze film damper are coupled with transfer functions and the vibration on the housings is predicted. The vibration response under single and multi-plane unbalances correlates very well with test data from turbocharger unbalance masters. The prediction model allows a thorough understanding of ball bearing turbocharger vibration on a high speed balancer, thus optimizing the dynamic behavior of the "turbocharger-high speed balancer" structural system for better rotordynamics performance identification and selection of the appropriate balancing process at the development stage of the turbocharger.

Keywords: Turbocharger / ball bearing / rotordynamics / high speed balancing / vibration management

1 Introduction

It is well known that high speed automotive turbochargers are sources of high vibration level on vehicles. Moreover, the bearing behavior nonlinearities makes their spectrum very complex including synchronous vibration, self-excited oil whirl and oil whip phenomena, subharmonics, superharmonics, combination frequencies and jump phenomena [4]. On [2] Gjika et al. did a critical analysis of different turbocharger vibro-acoustics mechanisms and sources as per Garrett's experience. There are outlined 9 noise types, which cover a full audible frequency range from 0 to 20000 Hz. Their sources can be rotordynamics or aerodynamics, and the transfer paths structural or gaseous. The turbocharger rotor-bearing system concept & design, assembling & balancing processes, housings and vehicle vibro-acoustics management are becoming a real challenge for both turbocharger manufacturers and OEMs.

Many researches have investigated the vibration interaction between bearing system rotordynamics and housings dynamics [1–13].

Foundation dynamics characteristics can be very well represented by frequency response functions (FRF), which can be obtained by finite element (FE) analysis or test; their quality is a fundamental step on mechanical vibration investigation.

* e-mail: kostandin.gjika@garrettmotion.com

Cavalca et al. [5] identified the influence of support flexibility on rotordynamics unbalance response; both rotor-bearing system and foundation have been modeled by finite elements. Dakel et al. [6] predicted the rotordynamics performances of a flexible rotor (symmetric and asymmetric) under masse unbalance combined with rigid base excitations; the stability chart, Campbell diagrams, steady-state responses as well as orbits of the rotor are analyzed. On [7] Ewins described how to obtain high quality of experimental FRFs and Yamaguchi et al. [8] made the best use of Fast Fourier Transformation (FFTs) approach on measured FRFs. Nicholas et al. [9] developed a concept of equivalent bearing coefficients based on the combination of experimental foundation FRFs with bearing force coefficients and used that on a rotordynamics code for predicting the critical speed. Xu and Vance [10] improved the model by refining the foundation modal damping from test data. Both studies demonstrated the impact of the flexible foundation on rotor-bearing system critical speed, validated by test data. Vazquez et al. [11,12] analyzed the rotordynamics performance of a three-disc rotor supported by two fluid film bearings on flexible anisotropic supports; the experimental FRFs were used to identify the characteristics of the foundations, an equivalent stiffness matrix was developed, and the damping was considered to be zero; the prediction of the first two critical speeds and of the threshold speed of instability correlates well with the test data. Shaposhnikov et al. [13] suggested a hybrid rotor-foundation model for a 2MW gas turbine engine, which has a very complex support structure. The rotordynamics has been modeled by finite elements and the foundation characteristics (direct, cross-coupling and cross talk dynamic stiffness and damping) obtained experimentally have been integrated into that. It shows better accuracy prediction of the critical speeds and support structural resonances.

A finite element analysis of a turbomachine which integrates in a single model the bearing system rotordynamics and the support dynamics can also be used for vibration performance prediction, but it seems to be costly and time consuming for foundation structures that are complex or have nonlinear behavior [9].

This paper describes a prediction model and validation aspects for the synchronous forced vibration of ball bearing turbocharger housings, but which can be applied to any other ball bearing turbomachine.

2 Automotive turbocharger description

Garrett-Advancing Motion considers the bearing system as the heart of the turbocharger. As part of continuous improvement and OEMs needs they have developed different technologies such as fluid bearings and ball bearings [1]. Advanced concepts such air foil bearing [14,15] are now implemented on Two-Stage Electric Compressor and the application on turbocharging technology is being validated.

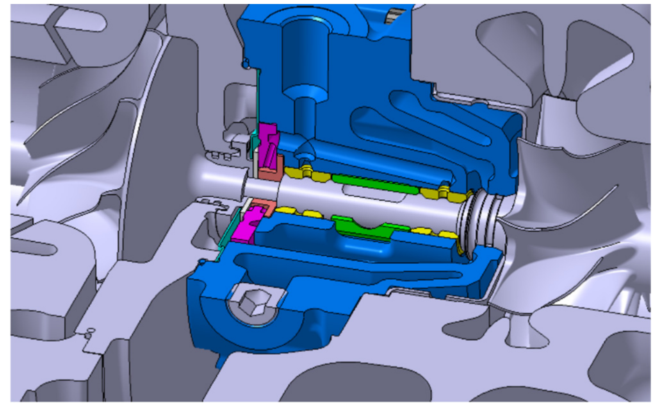

Fig. 1. Fully-floating fluid-bearing system.

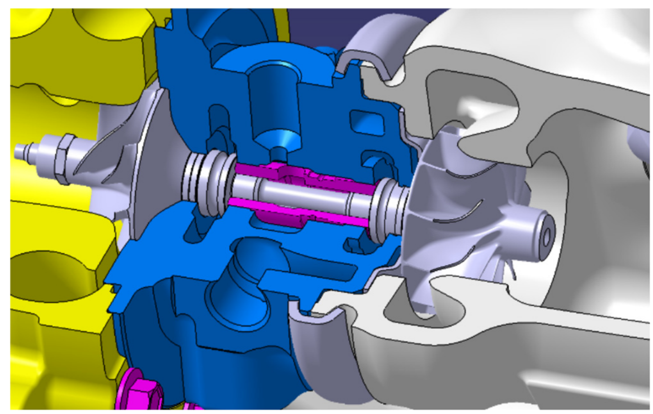

Fig. 2. Semi-floating fluid bearing system.

Figure 1 shows a fully-floating fluid bearing turbocharger. It is the original design, relatively low cost and still in production for commercial vehicle (CV) applications. That incorporates two oil films: the inner film between the shaft and the ring, and the outer one between the ring and the housing. Both behave as hydrodynamic films under unbalance forces. The axial load is supported by a separated hydrodynamic thrust bearing. Such a concept is known for its high damping, which reduces the shaft motion and vibration transmission on the housings. Gas stand shaft motion test is a good predictor of on-engine shaft motion behavior, but the high number of self-excitation frequencies (3 frequencies – inner film whirl, outer film whirl & ring speed) causes the design to be more susceptible to rotordynamics instability. It was found to be difficult to qualify shaft motion for small frame sizes.

Figure 2 presents Garrett's semi-floating fluid bearing with integrated thrust bearing that is successfully implemented on light vehicle (LV) turbochargers. Both bearings, compressor side and turbine side, are part of a single bushing, which is prevented from rotation by a pin; the inner oil film acts as hydrodynamic bearing and the outer film is behaving as squeeze film damper. The axial grooves on the bearing inside diameter serving oil on the thrust bearings while improving rotordynamics stability. It is a demonstrated design for very good rotordynamics

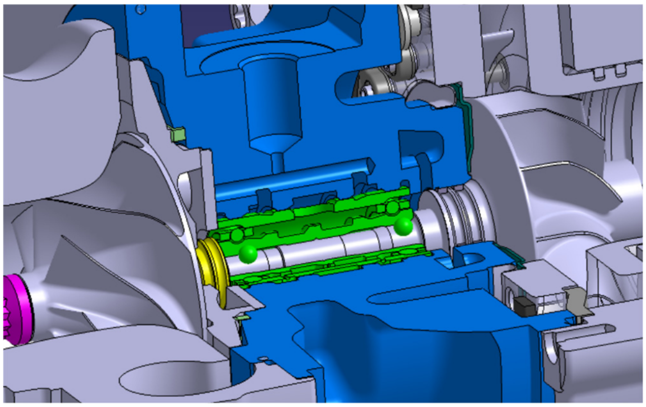

Fig. 3. Ball bearing system.

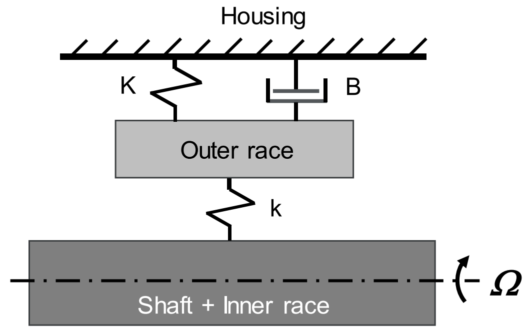

Fig. 4. Ball bearing squeeze film damper modeling.

stability due to the squeeze film damper, low radial power losses due to the small journal diameter and low vibration transmission due to the slender shaft design.

Figure 3 describes a conventional ball bearing cartridge turbocharger for LV and CV applications. The cartridge inner race is press fitted on the shaft and the outer race is prevented from rotating by a pin; the outer oil film behaves as squeeze film damper. This design shows very low power loss for improved fuel economy and transient performance, as well as excellent cold start behavior; Garrett-Advancing Motion identified no shaft motion dynamic instability issues due to missing hydrodynamic oil film. High speed balancing performance is affected by high rotordynamics bearing loads related to the rotating group stiffness and initial unbalance due to the assembly process.

3 Synchronous vibration prediction method for high speed ball bearing turbomachinery

Three steps are integrated on the method.

A "ball bearing-squeeze film damper" model allows to predict the isotropic stiffness and damping coefficients as function of the eccentricity; they are integrated on a rotordynamics code for bearing loads prediction under unbalances; the eccentricity is updated by a converging iterative process.

The foundation transfer functions are obtained from a commercial FE code.

The forced vibration on the housing are calculated by coupling rotating bearing load with transfer functions.

3.1 "Ball bearing-squeeze film damper" modelling

The dynamic behavior of balls, Figure 4, is modeled by springs; the isotropic stiffness is calculated from Tedric Harris formulas [16], equation (1), and the damping is considered null.

$$k = 3.29 \times 10^7 z (d\Delta)^{0.5} \cos(\alpha)^{2.5} \tag{1}$$

with:

k, ball stiffness (N/m)
z, number of balls
d, ball diameter (mm)
Δ, radial deflection (mm)
α, contact angle (radian)

The deflection is calculated by the equation (2).

$$\Delta = 9.74 \times 10^{-6} (F_0/z)^{2/3} d^{-1/3} \cos(\alpha)^{-5/3} \tag{2}$$

where F_o, is the load acting on the outer squeeze film damper.

The squeeze film damper model is derived from the Osborne Reynolds equation for incompressible and synchronous fluid loading [1]. Both the balls and the squeeze film damper are assumed to support the same load (i.e. the cartridge outer race is massless) Thermal model is considered adiabatic and viscosity/temperature is described by Walther's formula [17]. The bearing is assumed infinitely short and the oil film pressure is modeled as a cavitated π film model. The stiffness and damping coefficients can be calculated respectively by equations (3) and (4).

$$K = \frac{\pi \mu R L^3 N_{eff}}{30 {c_r}^3} \left(\frac{\varepsilon}{(1-\varepsilon^2)^2} \right) \tag{3}$$

$$B = \frac{\pi \mu R L^3 N_{eff}}{4 {c_r}^3 N_S} \left(\frac{1}{(1-\varepsilon^2)^{1.5}} \right) \tag{4}$$

where:

μ, fluid viscosity
R, journal radius
L, bearing length
c_r, radial bearing clearance
ε, eccentricity ratio
N_s, shaft speed (rpm)
$N_{eff} = |2N_{load} - N_{journal}|$, effective speed [18,19]

For a non-rotating bearing (case of the squeeze film damper), $N_{journal} = 0$ and for unbalance loading, $N_{load} = N_s$, then $N_{eff}/N_s = 2N_s/N_s = 2$.

3.2 Rotordynamics and bearing load modelling

The fundamentals of rotordynamics and the associated finite element code are presented at [20]; the equations (5), which govern the synchronous phenomena are detailed in [1].

$$[M]\{\ddot{\delta}\} + [C]\{\dot{\delta}\} + \Omega[G]\{\dot{\delta}\} + [K]\{\delta\} \ = \{F_{unb}(\Omega t)\} \tag{5}$$

where $\{F_{unb}(\Omega t)\}$ is the mass unbalance vector.

The rotating bearing loads can be presented by the formulas (6).

$$\begin{aligned}(F_{brg})_x &= F_{brg}e^{i\Omega t}\\ (F_{brg})_y &= F_{brg}e^{(i\Omega t+\pi/2)}\end{aligned} \tag{6}$$

where:

F_{brg}, bearing load magnitude
Ω, rotor speed (rad/s)

Depending on the distribution of unbalances on the rotating group, the load vectors on each of the bearings can be different in magnitude and phase. In case of two bearings they can be presented with the equations (7) and (8) where Φ is the phase angle between load vectors on the bearings.

$$\begin{aligned}\left(F_{brg_1}\right)_x &= F_{brg_1}e^{i\Omega t}\\ \left(F_{brg_1}\right)_y &= F_{brg_1}e^{(i\Omega t+\pi/2)}\end{aligned} \tag{7}$$

$$\begin{aligned}\left(F_{brg_2}\right)_x &= F_{brg_2}e^{(i\Omega t+\Phi)}\\ \left(F_{brg_2}\right)_y &= F_{brg_2}e^{(i\Omega t+\pi/2+\Phi)}\end{aligned} \tag{8}$$

3.3 Housings vibration modelling

The structural dynamics of housings can be modeled by any commercial FE prediction code. In this study ANSYS code [21] is used, and the fundamentals of modelling are presented on [1].

For modelling purposes, the OD (squeeze film damper clearance) bearing loads are applied to two dummy nodes on each bearing locations, featuring two lump mass elements with negligible mass, which are connected to the housing bore by constraint equations. The housing transfer functions are predicted by applying a rotating bearing load unit on each of dummy nodes. The coupling of the dynamic bearing loads with transfer functions allows to predict vibration on the housings.

4 Case study: ball bearing turbocharger vibration management on high speed balancer

Figure 5 shows a high speed balancer (HSB) for automotive turbocharger. A ball bearing CHRA (center housing rotating assembly) unbalance master, which allows the implementation of unbalances by using small metallic screws, is clamped on the mechanical tooling. The vibrations of the "CHRA-HSB" assembly are measured by an accelerometer implemented on the HSB fixture.

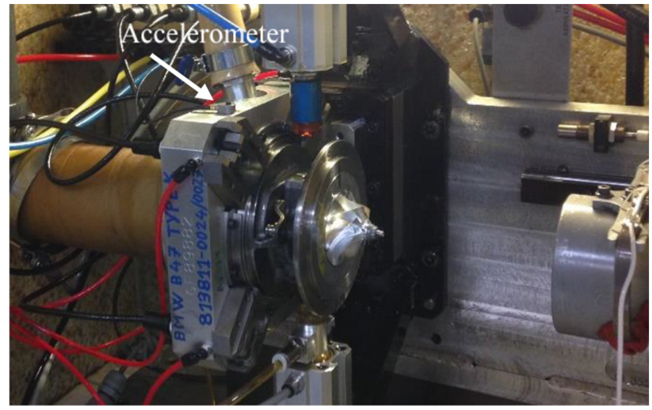

Fig. 5. Turbocharger unbalance master on HSB.

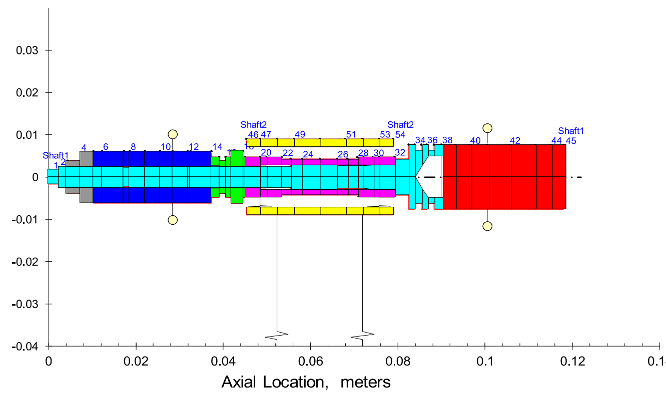

Fig. 6. Turbocharger rotordynamics model.

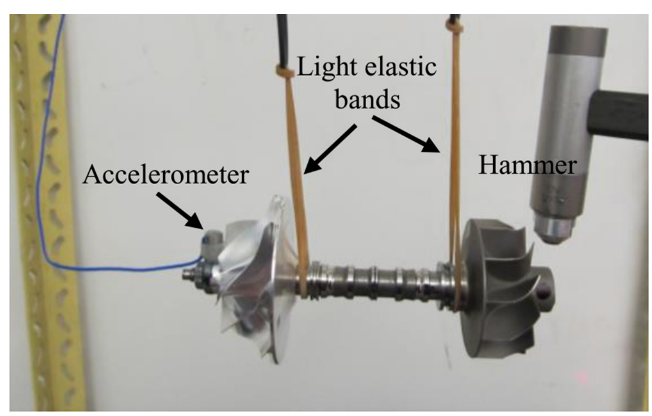

Fig. 7. Turbocharger rotating group on light elastic bands.

4.1 Turbocharger rotordynamics

The structural rotordynamics model of a ball bearing turbocharger is presented in Figure 6. It includes 44 beam finite elements for the rotating group and 8 for the bearing outer race; the wheel inertia characteristics are attached on their center of inertia; the balls and squeeze film damper are respectively modeled by springs and oil stiffness & damping coefficients.

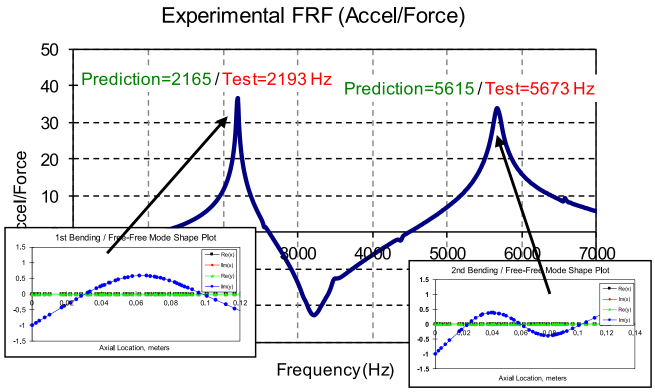

Fig. 8. Rotating group free-free natural frequencies and associated mode shapes. Test/prediction.

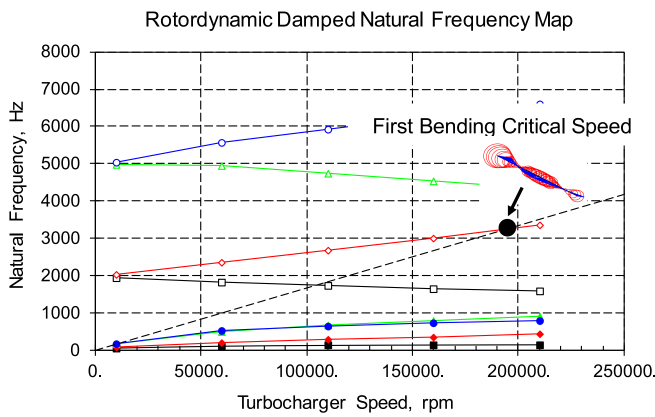

Fig. 9. Campell diagram.

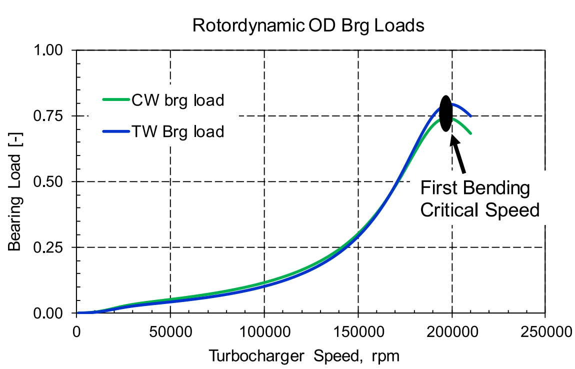

Fig. 10. Rotodynamics od bearing loads.

4.2 Free-free rotordynamics

Figure 7 shows how the experimental transfer functions (γ/F) of free-free rotating group are obtained; Figure 8 demonstrates good test/prediction correlation of natural frequencies that occur up to 7000 Hz.

4.3 Rotordynamics on HSB operation condition

Figures 9 and 10 summarize respectively the prediction of the Campbell diagram and OD bearing loads on the speed range up to 210000 rpm; bearing stiffness and damping coefficients are calculated for the converged eccentricity and the housings support is considered rigid. The first bending critical speed occurs at 186000 rpm.

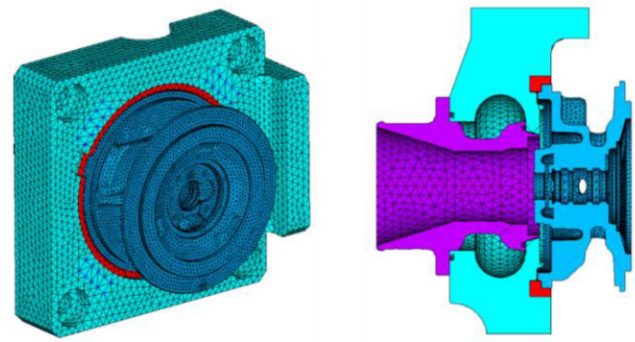

Fig. 11. Finite element model of "CHRA-HSB" housings.

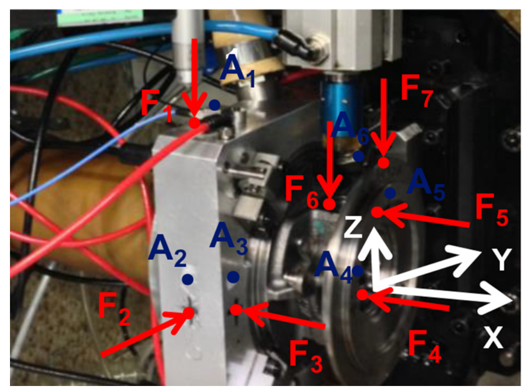

Fig. 12. Experimental vibration identification of "CHRA-HSB" structure.

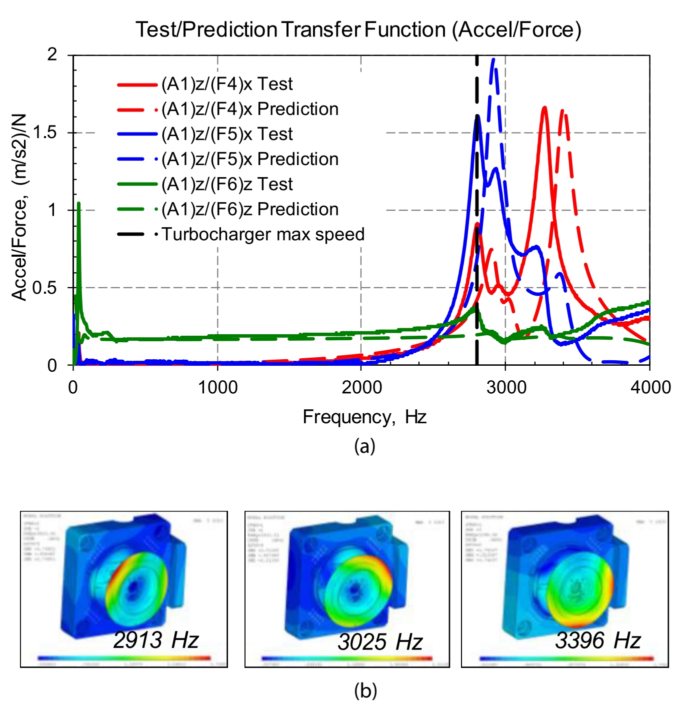

Fig. 13. "CHRA-HSB" modal analysis. (a) Transfer function. (b) Mode shapes.

Fig. 14. Turbocharger unbalance master.

4.4 "CHRA housing - HSB fixture" modal analysis

Figure 11 presents the finite element model of "CHRA housing – HBS fixture", which is validated by test/prediction transfer functions up to 4000 Hz (Figs. 12 and 13). At high speed range the turbocharger vibration response can be affected by the natural frequency at 2913 Hz.

4.5 Turbocharger vibration on HSB

CHRAs unbalance masters, which is shown in Figure 14, with ODmin, ODmax and ODnom squeeze film damper clearances were run on the high-speed balancer. Test masses have been implemented on different rotor planes (CWnose, CWface, TWface and TWnose) by using small screws and the vibration responses under different unbalance configurations have been collected by the accelerometer on the HSB fixture (see Fig. 4). Figure 15

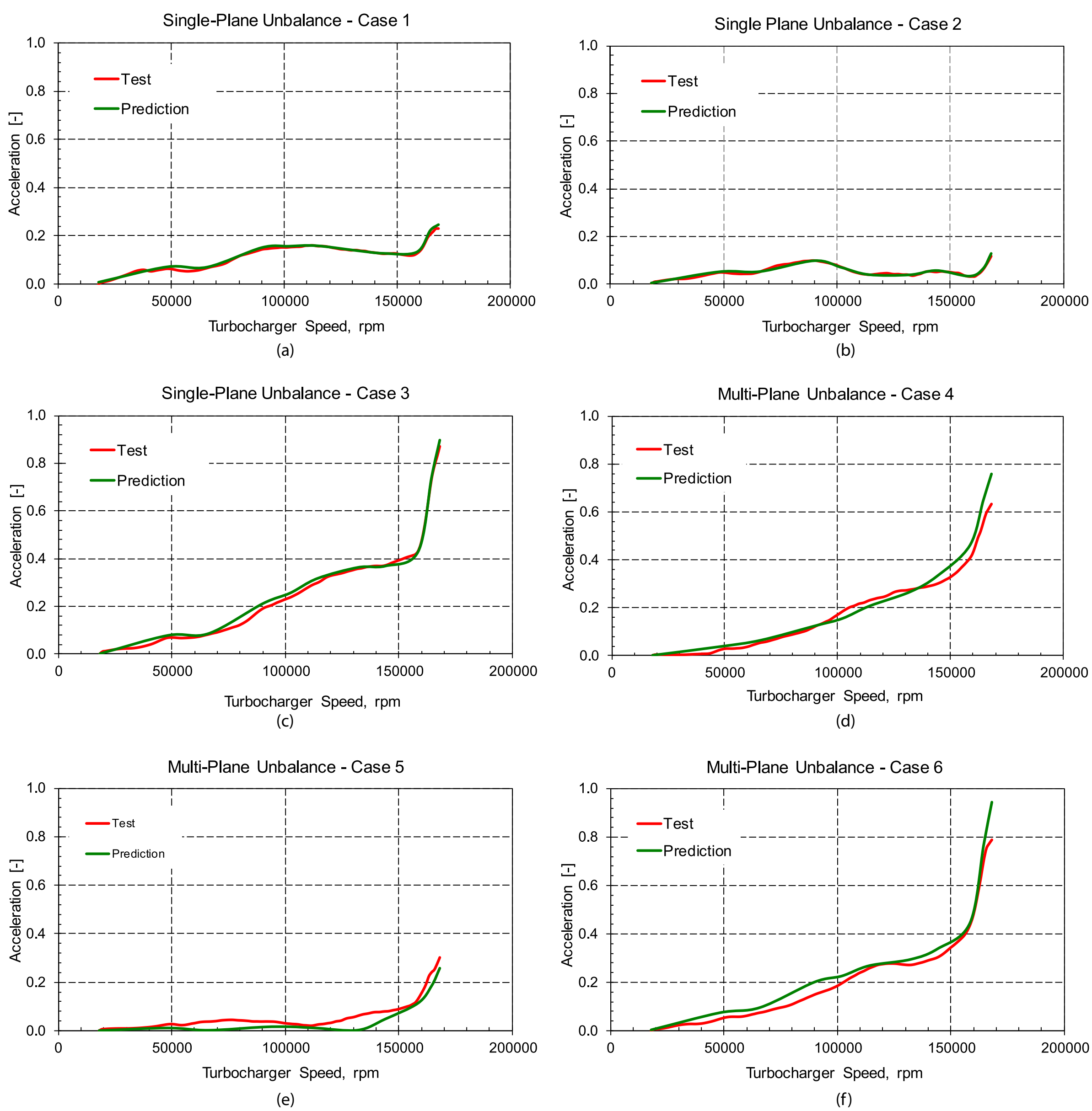

Fig. 15. Turbocharger vibration response: test/prediction (dimensionless).

summarizes 6 cases of test/prediction dimensionless responses; it shows good correlation. The vibration prediction model is validated.

5 Conclusion

The paper describes a prediction method for synchronous vibration management of ball bearing turbomachines; it is a continuation of the papers [1–3].

A model and the associated prediction code for the static and dynamic behavior performance of "ball bearing cartridge-squeeze film damper" are developed. The dynamic behavior of the balls is modeled with Tedric Harris formulas and the squeeze film damper characteristics derive from the Osborne Reynolds equation; the stiffness and damping coefficients are used on a rotordynamics code to predict the bearing loads by converging with the bearing system eccentricity ratio; the OD rotating bearing loads are coupled with foundation transfer functions predicted by FE analysis and the vibration on the housing are predicted.

The approach is validated with numerous test data from a Garrett's ball bearing turbocharger on the high-speed balancer, but it is generic and can be applied to any turbomachinery.

The next step consists in the validation of the method on vehicle operating conditions.

Nomenclature

B	Squeeze film damping
$[C]$	"Shaft-bearing" damping matrix
c_r	Radial bearing clearance
CHRA	Center housing rotating assembly
CV	Commercial vehicle
d	Ball diameter
Δ	Ball radial deflection
F_{brg}	Bearing load
FE	Finite element
FRF	Frequency response function
$\{F_{unb}(\Omega t)\}$	Mass unbalance force vector
$[G]$	Gyroscopic matrix
HSB	High speed balancer
i	Imaginary unit
k	Ball stiffness
K	Squeeze film stiffness coefficient
$[K]$	"Shaft-bearing" stiffness matrix
L	Bearing length
LV	Light vehicle
$[M]$	"Shaft-discs-bearing" inertia matrix
N_{eff}	Effective speed
N_L	Load speed
N_s	Shaft speed
OD	Squeeze film damper clearance
R	Journal radius
t	Time
z	Number of balls
$\{\delta\}, \{\dot{\delta}\}, \{\ddot{\delta}\}$	Global DOF vectors (displacement, velocity and acceleration)
α	Contact angle
ε	Eccentricity ratio
Φ	Phase difference between compressor side and turbine side bearings load vectors
μ	Fluid viscosity
Ω	Rotational speed

Subscripts

brg	Bearing (bearing load)
eff	Effective (effective speed)
min, max	Minimum, maximum (bearing clearance)
unb	Mass unbalance
r	Radial (radial clearance)

The authors are indebted to Garrett Advancing Motion for permission to publish this work.

References

[1] K. Gjika, P. Mahadevan, A. Costeux, Turbocharger synchronous vibration control on high speed balancer. Test and prediction, ASME Journal of Engineering for Gas Turbines and Power **136**, 071603 (2014)

[2] K. Gjika, A. Costeux, P. Mahadevan, W. Meacham, L. Stuart, G. Gaude, VUCT – a consolidated product–process approach for DFM, balancing technology performance and vibration control on vehicle, The Exponent **6**, (2014)

[3] J. Wilson, F. Daguin, G. Gaude, K. Gjika, P. Francois, P. Talbert, Turbocharger noise: a continuous challenge, The Exponent **6**, (2014)

[4] B. Schweizer, M. Sievert, Nonlinear oscillations of automotive turbocharger turbine, Journal of Sound and Vibration **321**, 955–975 (2009)

[5] K.L. Cavalca, P.F. Cavalcante, E.P. Okabe, An investigation on the influence of the supporting structure on the dynamics of the rotor system, Mechanical Systems and Signal Processing **19**, 157–174 (2005)

[6] M. Dakel, S. Baguet, R. Dufour, Steady-state dynamic behavior of an on-board rotor under combined base motions, Journal of Vibration and Control **20**, 2254–2287 (2014)

[7] D.J. Ewins, Modal testing: theory and practice, *Research Studies* Press LTD., Letchworth Hertfordshire, England, 1984

[8] T. Yamaguchi, M. Ogawa, T. Kasahara, N. Arakawa, Advanced measurement method of frequency response function, *Proceedings of the 3rd International Modal Analysis Conference*, Orlando, Florida, Volume I, pp. 565–568, 1985

[9] J.C. Nicholas, J.K. Whalen, S.D. Franklin, Improving critical speed calculations using flexible bearing support FRF compliance data, *Proceedings of the 15th Turbomachinery Symposium*, Texas A&M University, College Station, TX, 1986

[10] J. Xu, J.M. Vance, Experimental determination of rotor foundation parameters for improved critical speed predictions, ASME Paper No. 97-GT-449, 1997

[11] J.A. Vazquez, L.E. Barrett, R.D. Flack, Including the effects of flexible bearing supports in rotating machinery, International Journal of Rotating Machinery **7**, 223–236 (2001)

[12] J.A. Vazquez, L.E. Barrett, R.D. Flack, Flexible bearing supports, using experimental data, Journal of Engineering for Gas Turbines and Power **124**, 369 (2002)

[13] K. Shaposhnikov, X. Wu, C. Gao, Influence of foundation and support structure elasticity on rotordynamics of 2 MW gas turbine engine, *Proceedings of the International Gas Turbine Congress* 2019, Tokyo

[14] K. Gjika, Turbocharger bearing systems technology – challenges and strategic developments, Garrett Booster Magazine, pp. 6–11 (2003)

[15] G. LaRue et al., Turbocharger with hydrodynamic foil bearings, United States Patent No: US 7, 108, 488 B2, 2006

[16] T.A. Harris, M.N. Kotzalas, Rolling bearing analysis, 5th edition, CRC Press, Boca Baton, Florida, 2006

[17] M. Sánchez-Rubio, F. Chinas-Castillo, F. Ruiz-Aquino, J. Lara-Romero, A new focus on the Walther equation for lubricant viscosity determination, Lubrication Science **18**, 95–108 (2006)

[18] O. Pinkus, B. Sternlicht, Theory of hydrodynamic lubrication, McGraw-Hill Book Company, Inc., New York, 1961

[19] J.M. Stone, A.F. Underwood, Load carrying capacity of journal bearings, SAE Quarterly Transactions **1**, 56–70 (1947)

[20] D. Childs, Turbomachinery rotordynamics, D. John Wiley & Sons, Inc., NY, 1993

[21] ANSYS 2020 release 1, https://www.ansys.com/fr-fr/products/release-highlights

Cite this article as: K. Gjika, A. Costeux, G. LaRue, J. Wilson, Ball bearing turbocharger vibration management: application on high speed balancer, Mechanics & Industry **21**, 619 (2020)